Nature Environment and Pollution Technology
An International Quarterly Scientific Journal

p-ISSN: 0972-6268
(Print copies up to 2016)
e-ISSN: 2395-3454

Vol. 24 | No. 2 | Article ID D1701 | 2025

Original Research Paper

https://doi.org/10.46488/NEPT.2025.v24i02.D1701

Open Access Journal

Mapping of Groundwater Potential Zones Using Fuzzy Logic Technique at Kadamaian Basin, Kota Belud, Sabah, Malaysia

Evienstein Wilfred† and Zulherry Isnain
Faculty of Science and Natural Resources, Universiti Malaysia Sabah, Jalan UMS, 88400 Kota Kinabalu, Sabah, Malaysia
†Corresponding author: Evienstein Wilfred; evienstein@gmail.com

Abbreviation: Nat. Env. & Poll. Technol.
Website: www.neptjournal.com

Received: 13-07-2024
Revised: 04-09-2024
Accepted: 10-09-2024

Key Words:
GIS
Fuzzy logic
Groundwater potential
Mapping

Citation for the Paper:

Wilfred, E. and Isnain, Z., 2025. Mapping of groundwater potential zones using fuzzy logic technique at Kadamaian basin, Kota Belud, Sabah, Malaysia. *Nature Environment and Pollution Technology,* 24(2), D1701. https://doi.org/10.46488/NEPT.2025.v24i02.D1701

Note: From year 2025, the journal uses Article ID instead of page numbers in citation of the published articles.

Copyright: © 2025 by the authors
Licensee: Technoscience Publications
This article is an open access article distributed under the terms and conditions of the Creative Commons Attribution (CC BY) license (https://creativecommons.org/licenses/by/4.0/).

ABSTRACT

This research was initiated to study the groundwater potential zones using the Fuzzy logic technique at Lembangan Kadamaian, Kota Belud, Sabah, and its surroundings. The lithological units of this study mainly focus on the sedimentary rock of Wariu Formation, Crocker Formation, and Trusmadi Formation, including the quaternary alluvium deposition unit of Kota Belud. Based on the structural geology analysis results, the deformation trends are in the northwest-southeast direction. The interpretation of groundwater potential zones was made by using the ArcGIS Pro, R-studio Global Mapper, and several other mapping-related software. Ten thematic maps that have been produced are lithological map, lineament density map, rainfall map, distant from river map, distant from lineament map, drainage density map, landform, and land cover map, Topographic Wetness Index (TWI) map, rock porosity map, curvature map, and slope steepness map. GIS techniques were used during the spatial analysis stage. All thematic maps have their class values and are based on field data, relevant department data, and remote sensing data. Further processes were done using R-studio, Fuzzy Toolset, and Raster Calculator. This process afterward will produce the groundwater potential map of the study area. The final result has been supported by the data of tube wells from the Department of Minerals and Geosciences, Sabah, and was validated using the ROC and AUC curve validation technique.

INTRODUCTION

Background

This research focuses on delineating the zones with high potential for groundwater within the study area at Lembangan Kadamaian, Kota Belud, and Sabah. However, This research also includes preliminary parts such as general geology that cover some aspects of geography, geomorphology, stratigraphy, rock petrography, water quality, and structural geology. Meanwhile, the main objective of the research was continued in mapping techniques on the groundwater potential through the fuzzy logic technique by using the ArcGIS Pro and R-studio software.

The study area can be found in the western part of Sabah. The study area consists mainly of the Crocker Formation, Wariu Formation, and Pleistocene alluvium deposition unit (Fatin et al. 2022) and other rock units such as Trusmadi Formation, basic igneous, crystalline basement, plutonic igneous, Pleistocene alluvium deposit, and chert-spilite formation. The study area distance from the Kota Kinabalu, the capital state of Sabah was about 73 km. The area of the study area covers around 848.4 km^2. The coordinates of the study area are 116°21’0” E - 116°41’0” E and 6°26’0” N - 6°0’0” N (Fig. 1).

The Fuzzy Logic Technique used during the analysis is based on the probability of a phenomenon occurring within a spectrum from 0 to 1 without requiring the assumption of normality for predictor variables (Assimakopoulos et al. 2023).

Studies were carried out based on existing data such as well data, fieldwork data, geological maps, satellite images, and topography maps.

Geological Settings

The South China Sea is a prominent feature in the Southeast Asian region, and numerous models have been developed to depict the evolution occurring in that region (Balaguru et al. 2023). However, this study mostly discusses tectonic evolution within the scope of the study area, which is in the Northwest Sabah region located southeast of the South China Sea Basin.

Generally, Sabah is encircled by active tectonic plates such as the Indo-Australian Plate, Philippine Plate, Pacific Plate, and Eurasian Plate. Sabah's location is in the northern part of the Borneo island, which is often influenced by various tectonic events triggered by these active plates. Fig. 2 shows the major plates surrounding Sabah.

Ghaheri et al. (2017) stated that the seas surrounding Sabah, such as the Sulu Sea, Celebes Sea, and South China Sea, greatly influence tectonic events in Sabah. The existence of basins in the Sulu Sea subduction zone, the Celebes Sea subduction zone, and the South China Sea spreading zone is caused by tectonic events occurring in the region (Fig. 2).

The stratigraphy of the study area is closely related to the regional stratigraphy found in the western part of Sabah. According to Tongkul (1991), sedimentary rocks and igneous

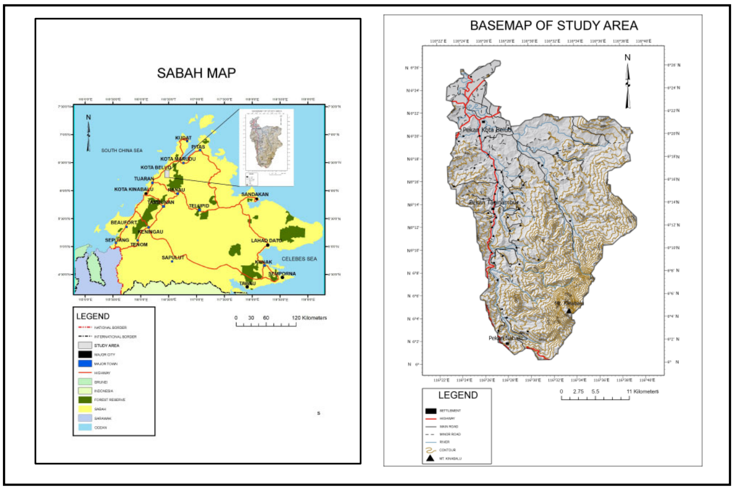

Fig. 1: Map showing the base map of the study area.

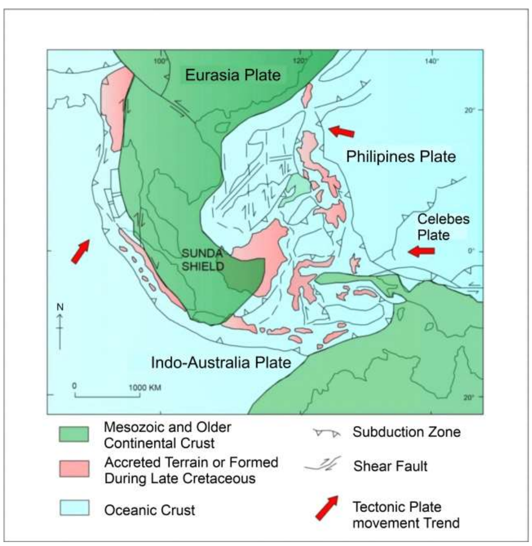

Fig. 2: Main tectonic plate of Southeast Asia. (Source: Modified from Tan & Lamy (1990))

rocks associated with metamorphic rocks were mostly found in the western and northern parts of Sabah. Sedimentary rocks are dominated by sandstone with shale and associated with chert, limestone, and conglomerate. Meanwhile, igneous rocks consist of serpentine, basalt/sphilite, agglomerate, gabbro, dolerite, andesite, granodiorite, and adamellite. Metamorphic rocks consist of hornblende schist and gneiss. The correlation between all these rock formations can be seen in Fig. 3.

According to Basir (1988), the oldest sedimentary rock in the region is radiolarian chert from the early Cretaceous age. These thin layers of chert can be associated with basic igneous rocks such as basaltic or spilit. There are also several types associated with these two rock types, namely peridotite and ultrabasic serpentine, intrusive dolerite, and metamorphic hornblende, schist, and gneiss. These rock associations depict an ophiolite sequence representing the Mesozoic oceanic crust that forms the region's basement rocks.

The basement rocks are overlain by sedimentary formations, including the Crocker Formation, Trusmadi Formation, and Wariu Formation, which range in age from Eocene to mid-Miocene. The western part of Sabah is primarily characterized by the Crocker and Trusmadi formations, both of which are deep-sea sediments characterized by alternating layers of sandstone and shale (Tongkul 1991). The Wariu Formation, on the other hand, is a mixed sediment deposit consisting of various-sized clasts such as mudstone, greenish arenite, coarse-grained arenite, metaklastic, micritic limestone, and shiny greenish argillite, which date back to the Middle Miocene (Tijia 1988).

The intrusive igneous rocks, such as Mount Kinabalu and the extrusive volcanic rocks of Sirar Volcanic Island, were formed during the Miocene-Pliocene age (Tongkul 1991).

Based on the geological map in Fig. 4, which was created by referring to the Sabah Geological Map 4th Edition (JMG 2010). The main rock unit in the study consists of the Wariu Formation, Crocker Formation, and Quaternary Coastal Alluvium (Fatin et al. 2022), followed by small portions of the Trusmadi Formation, basic igneous rocks, faulted basement, plutonic igneous rocks, Pleistocene river alluvium deposits, and chert-sphilite. Observations were made through field studies aimed at distinguishing and confirming the presence of rock units and their characteristics in the study area.

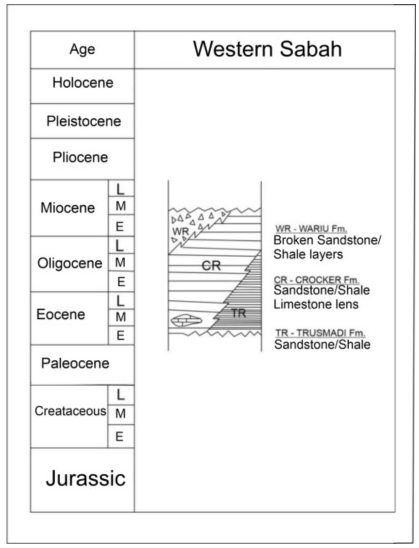

Fig. 3: general stratigraphy of western Sabah. (Source. Modified from Tongkul (1991))

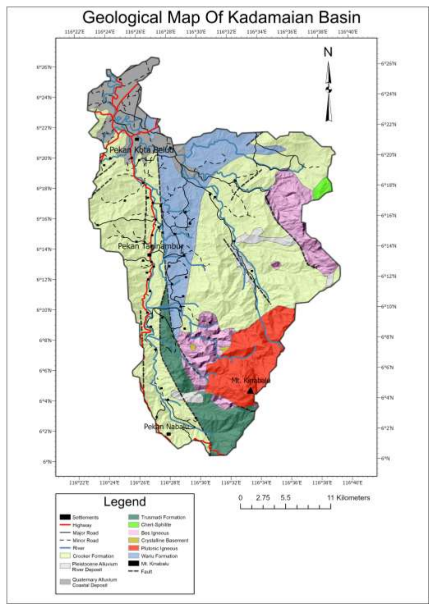

Fig. 4: The geological map of the study area in the Kadamaian Basin, Kota Belud. (Source: Sabah Geological Map 4th Edition (JMG, 2010))

MATERIALS AND METHODS

Fuzzy Logic Technique

The fuzzy logic technique has been applied in various fields, such as in mineral prospectivity (Zhang et al. 2017), environmental risk assessment mapping (Poberezhna et al. 2022), soil erosion prediction (Mitra et al.1998), and forest fire risk mapping (Juvanhol R.S> 2021). Introduced by Zadeh (1996), Fuzzy Logic consists of objects in a set that have their own degrees of membership where each thematic map was reclassified and assigned fuzzy logic membership values. These membership values are significant in defining the criteria for identifying groundwater potential zones in the study area. Assimakopoulos et al. (2003) state that the degrees of membership in the set vary between 0 (unsuitable or lowest groundwater potential) and 1 (most suitable or highest groundwater potential). All of the fuzzified thematic maps were then set to overlay each other using the ‘fuzzy overlay’ tool in ArcGIS Pro software. Fuzzy sum operators were used for the factor theme integration (Fig. 5). The product of the fuzzy logic overlay was then reclassified into five classes, ‘very poor’, ‘poor’, ‘moderate’, ‘high’, and ‘very high’ groundwater potential zones. Fuzzy subsets can be represented by the following membership functions;

$$\mu A : (x) \rightarrow [0,1]$$

The function can be associated with each parameter in a fuzzy set represented by $\mu A :(x)$. The value of X in $\mu A :(x)$ represents each parameter in a fuzzy set and its degree of membership. A value of 1 signifies a complete membership of a parameter, whereas a value closer to 0 indicates a weaker membership of that parameter in a fuzzy set (Kollias & Kalivas 1998).

Model Validation for Potential Zones of Groundwater

To guarantee the precision of prospective groundwater zone maps, the applicability of the methods used in this study for mapping groundwater zones was validated through the Receiver Operating Characteristic Curve (ROC) and Area Under the Curve (AUC) (Pourtaghi & Pourghasemi 2015, Ozdemir et al. 2011).

The AUC value in the ROC system, which goes from 0.5 to 1.0, is used to evaluate the model’s accuracy. An AUC of 0.5 would be assigned to a model that only characterizes or forecasts the existence of a groundwater zone. According to Pourghasemi et al. (2012), a graphical representation of the ROC curve is created by plotting the false-positive rate (1-specificity) on the X-axis and the true positive rate (sensitivity) on the Y-axis.

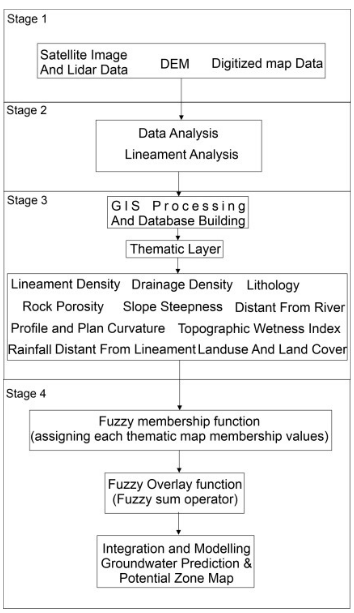

Fig. 5: The pathway of combining the fuzzy logic technique and GIS in this study.

RESULTS AND DISCUSSION

The fuzzy membership values will be organized in tabular form, and their computation will be carried out using the Raster Calculator and Fuzzy Toolset available in the ArcGIS Pro software. Table 1 shows the statistical data of parameters according to the classes used in this study. The fuzzy membership values were generated through the fuzzyfication toolset in ArcGIS Pro. Below is the formula for the fuzzy logic function used in computing the fuzzy membership for the dataset;

Linear Membership Function

The linear membership function refers to the relationship between input and output values represented by a linear equation where the membership values in a fuzzy set increase and decrease linearly with the variable. The linear fuzzy function is represented through the following equation:

$$\mu(y) = m \times x + b$$

Where,

$\mu(y)$ = membership value of the output fuzzy set (y),

x = input value,

m = slope of the linear function,

b = intercept (or offset).

Gaussian Membership Function

The Gaussian membership function is represented by the Gaussian curve shape, characterized by its mean and standard deviation. This function is used to model uncertainty in the real world, where elements can be part of a set. The Gaussian membership function is widely used in fuzzy logic systems. The following equation represents the Gaussian fuzzy function:

$$\mu(x) = \exp(-(x - c)^2 / (2 \times \sigma^2))$$

Where,

x = input value for which the membership value is to be determined.

c = center or mean of the Gaussian curve, representing the most likely value for full membership.

σ = standard deviation, which controls the spread or width of the curve. A larger σ value produces a wider curve and lower peak.

Table 1: Fuzzy membership values for each parameter class in this study.

Parameters	Class	Fuzzy Type	Fuzzy Membership Value
Lineament density	0-0.500	Gaussian	0.79
	0.500-1.000		0.85
	1.000-1.500		0.9
	1.500-2.000		0.95
	2.000-2.600		1
Drainage Density	0-0.5	Linear	1
	0.5-1		0.83
	1-1.5		0.66
	1.5-2		0.5
	2-2.5		0.14
Distance From Drainage	0-400	Linear	1
	400-800		0.82
	800-1200		0.69
	1200-1700		0.55
	1700-2400		0.42
	> 2400		0
Rock Porosity	≤ 10	Gaussian	0
	$\geq 11 \leq 20$		0.25
	$\geq 21 \leq 30$		0.50
	$\geq 31 \leq 45$		0.75
	≥ 46		1
Distance From Lineament	0 - 200	Linear	1
	200 - 400		0.81
	400 - 600		0.62
	600 - 800		0.44
	>800		0
Slope Steepness	≤ 6	Linear	1
	6 - 11		0.76
	11 -18		0.52
	18 - 25		0.29
	≥ 50		0
Profile and Plan Curvature	Convex	Gaussian	0
	Flat		0.5
	Concave		1
Rainfall	< 3600	Gaussian	0
	3600 - 3700		0.26
	3700 - 3800		0.50
	3800 - 3900		0.74
	> 3900		1
Landuse And Land Cover (LULC)	Water Body	Linear	1
	Agriculture		1
	Shrubs		0.67
	Jungle		0.5
	Urban		0.33
	Barren Land		0
	Cloud Cover		0
Lithology	Coastal River Alluvial Deposits	Linear	1
	Pleistocene River Alluvial Deposits		1
	Crocker Formation		0.66
	Wariu Formation		0.66
	Trusmadi Formation		0.22
	Chert-Sphilite		0
	Basic Igneous		0
	Plutonic Igneous		0
	Crystalline Basement		0
Topographic Wetness Index(TWI)	< 5	Gaussian	0
	5		0.14
	6		0.23
	7		0.33
	> 7		1

In this function, as x moves away from the center c, the membership value gradually decreases, indicating the degree of membership of x in that fuzzy set.

Groundwater Potential Suitability Analysis

The production of groundwater potential maps through this method involves the use of a raster calculator and Fuzzy toolset found in the ArcGIS Pro software by combining the fuzzified thematic map for each of the parameters used in this study. Fig. 6 was the fuzzified thematic map for each of the parameters used in this research. The membership values were given through the fuzzy membership toolset in ArcGIS Pro.

Lithology vs. Groundwater Potential

In this study, thematic lithological layers are crucial in determining the groundwater potential within a particular

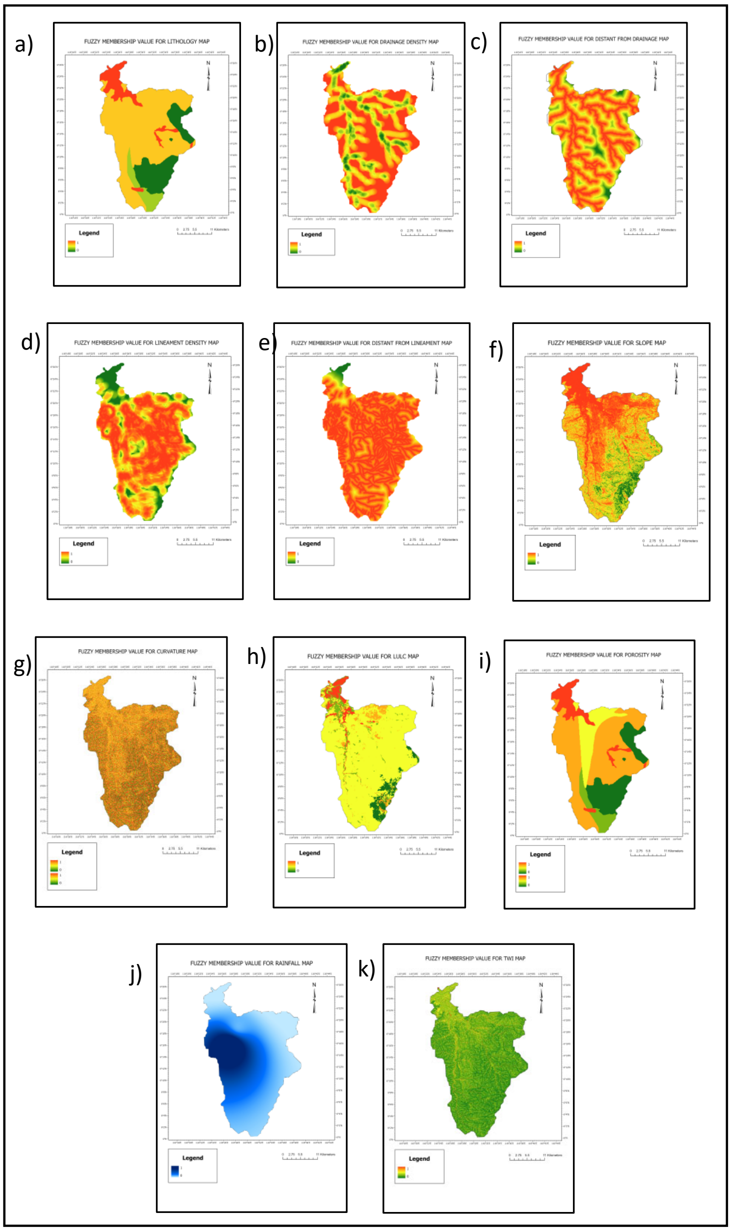

Fig. 6: a) Lithology map b) Drainage Density map c) Distance From Drainage map d) Lineament Density Map e) Distant From Lineament f) Slope Steepness map g) Curvature map h) Landuse and Land Cover map i) Rock Porosity map j) Rainfall map k) Topography Wetness Index map.

area. This is because the permeability and porosity of the layers at the surface affect the infiltration of surface runoff into the aquifer (Antenah et al. 2022, Melese & Belay 2022). The Crocker Formation, followed by rocks of the Wariu Formation and Quaternary coastal alluvial units, were the dominant rock units in the study area, comprising 52.60%, 13.07%, and 7.93% of the study area, respectively, and they have high potential to act as aquifers. In addition to these formations, there are also the Trusmadi Formation and Pleistocene river alluvial deposits, which respectively cover 6.24% and 1.89% of the study area and are also potential water-bearing units due to the presence of sandstone in these formations and the suitable characteristics of the Pleistocene river alluvial unit to act as an aquifer. Meanwhile, other rock units in the study area, such as igneous plutons, basaltic plutons, basement complex, and chert-spilite, had been categorized as having less potential to be an aquifer in this study. The fuzzfying process of this thematic map involved giving the highest membership value to alluvium quaternary and Pleistocene alluvial units, followed by the Crocker formation, Wariu formation, Trusmadi formation, Chert-sphilite rock unit, and the lowest membership value were shared between the igneous pluton, basaltic pluton, and basement complex (Fig. 6(a)).

Direct observations of well locations on the base map of the study area indicate that the majority of tube wells developed by the Department of Minerals and Geosciences, Sabah, are located in the sandstone of Crocker Formation, and Quaternary coastal alluvial areas (Fig. 7(a)).

Drainage Density vs Groundwater Potential

The drainage density map was created using the DEM (Digital Elevation Model) data, which was generated by Global Mapper software and was then processed in ArcGIS Pro through “line density” and “interpolation” features. According to the base map, the primary river branches in the study area are Sungai Wariu and Sungai Kadamaian, which flow from the northwest to the southeast of the study area.

According to Razandi et al. (2015), drainage density is inversely correlated to the permeability of an area. Other than that, an area with high drainage density shows that the area has low permeability, high angle of steepness, and high surface water runoff; meanwhile, an area with low drainage density is vice versa. In this study, areas with high flow density are associated with the rate of recharge and the capacity of surface water infiltration. Therefore, the hypothesis that high density in a particular location will increase the ability of recharge rate and surface water infiltration capacity into the groundwater system has been accepted for this study. The average flow density in the study area is 444.588 km.km^{-2}, based on calculations using the following formula;

$$\text{Average Drainage Density} = \frac{\sum_{1}^{n} Drainage\ Length}{Basin\ Area}$$

The thematic map of drainage density produced for this study is divided into five categories: very high (2.0 - 2.5 km.km^{-2}), high (1.5 - 2.0 km.km^{-2}), moderate (1.0 - 1.5 km.km^{-2}), low (0.5 - 1.0 km.km^{-2}), and very low (0 - 0.5 km.km^{-2}), each comprising 0.09%, 1.28%, 11.84%, 30.66%, and 56.30% of the study area’s total area (Fig. 7(b)). For the fuzzification process of the drainage density thematic map, the highest membership value was given to the very high density of drainage, and the lowest membership value was given to the very low drainage density (Fig. 6(b)).

Distance from Drainage vs Groundwater Potential

The distance from drainage and surface water flow can affect the groundwater recharge rate (Machiwal et al. 2011, Mallick et al. 2019, Adeyeye et al. 2019). According to Doke et al. (2021), the groundwater level is higher near drainage compared to areas far from it. The distance from drainage map data was obtained from the power.larc.nasa.gov website and was created using the Euclidean distance tool in ArcGIS Pro software. The resulting thematic map was divided into five classes: 0-400 m, 400-800 m, 800-1200 m, 1200-1700 m, 1700-2400 m, and > 2400 m (Fig. 7(c)). In the fuzzification process of the distance from the drainage thematic map, the lowest membership value was given to the farthest distance from the drainage, and the highest membership value was given to the nearest distance from the drainage (Fig. 6(c)).

Based on the comparison between well locations and the distance from the streams map, it was found that the majority of tube wells yielding significant groundwater findings, i.e., above 2 m^3.h^{-1}, are concentrated within the 0-400 m and 400-800 m range from the main drainage in the study area (Fig. 7(c)). This observation demonstrates that groundwater is directly influenced by these parameters.

Lineament Density vs Groundwater Potential

In this study, lineament density is a crucial feature in determining the groundwater potential of an area. Lineaments represent fractures, fissures, fault zones, and joints formed due to tectonic activities and stresses. These linear patterns can be defined as secondary porosity, which can influence the infiltration rate of surface recharge and runoff of groundwater aquifers.

High groundwater potential is associated with high lineament density (Magowe & Carr 1999, Hung et al. 2005, Al-Ruzouq et al. 2019). In this study, lineament data were obtained from the DEM (Digital Elevation Model) map, where linear patterns on the map were identified and then analyzed for lineament density using ArcGIS Pro software. The average density for the entire study area is 951.392 km^{-1} and was obtained through the following formula;

$$\text{Average Lineament Density} = \frac{\sum_1^n Lineament\ Length}{Basin\ Area}$$

The lineament density map generated through this analysis has been categorized into five classes: very low (0 - 0.5 km^{-1}), low (0.5-1.0 km^{-1}), moderate (1.0-1.5 km^{-1}), high (1.5-2.0 km^{-1}), and very high (2.0-2.6 km^{-1}) (Fig. 7(d)). The distribution of area percentages for each class in the study area was 22%, 33%, 30%, 13%, and 2%. Based on the thematic map in Fig. 7, the high to very high lineament density is concentrated in the soft rock areas of the Wariu Formation and Crocker Formation (Fig. 7(d)).

Distance from Lineament vs. Groundwater Potential

In hydrogeological research, the distance from lineaments is a crucial factor because prominent hydrogeological zones can be found near major lineament structures (Benjmel 2020). The lineament trace map in Fig. 7(f) shows dominant linear structures influencing rock units in the study area. Tectonic analysis indicates that the dominant stress direction in the study area is northwest-southeast. In this study, the thematic map of distance from lineaments can be categorized into five classes: 0 – 200 m (very low), 200-400 m (low), 400 m-600 m (moderate), 600 m-800 m (high), and > 800 m (very high) (Fig. 6(e) & Fig. 4(f)). In the fuzzification process of the thematic map, the nearest distance from the lineament was given a high membership value, while the farthest distance from the lineament was given the lowest membership value(Fig. 6(e)).

Slope vs Groundwater Potential

According to Ganapuram et al. (2009), slope steepness plays a role in influencing the presence and movement of both surface runoff and groundwater. Therefore, it can be said that slope steepness is a significant factor in infiltration and water flow.

Slope analysis in this study was conducted using the Slope Tools feature in ArcGIS Pro software. To generate thematic maps of slope steepness, raster DEM (Digital Elevation Model) data will be utilized. The assessment of groundwater potential in the study area will then be generated using the thematic layer of slope steepness as one of the crucial parameters in this study. This is because, through slope analysis, areas with high and low slopes can be identified, where in areas with steep slopes, rainfall-runoff flows more rapidly than in areas with gentle slopes. Thus, areas with steep slopes contribute less to groundwater recharge.

Based on Fig. 7(g), slope steepness in the study area has been divided into five classes: $\leq 6^\circ$ (very gentle slope), 6°-11° (gentle slope), 11°-18° (moderate), 18°-25° (steep), and $\geq 50^\circ$ (very steep), each comprising 16.67%, 14.53%, 21.54%, 19.95%, and 27.31% of the study area, respectively. Areas with very gentle and gentle slopes are located in the northwest and along the main streams in the study area, while steep and very steep areas are located in the southeast of the study area. In the fuzzified thematic map of this parameter, the most gentle slope was given a high membership value, and vice versa for the steepest slope (Fig. 6(f)).

Curvature vs. Groundwater Potential

A statement by Benjmel et al. (2022) said that curvature refers to the shape of the earth's surface and is used in the topographic analysis of an area. Thematic maps for curvature are generated using raster DEM data through ArcGIS Pro software. In this study, the curvature map generated is a combination of planar curvature and profile curvature values. The acceleration and deceleration of water flow are depicted by the profile curvature in the direction of the maximum slope gradient, while planar curvature affects the concavity and convexity of flow perpendicular to the slope gradient. A statement by Arulbalaji et al. (2019) said that the combination of these values could more accurately depict flow on the surface, where curvature is used in mapping groundwater potential to indicate groundwater flow direction and potential for groundwater recharge.

The curvature map in the study area is classified into three classes: concave, flat, and convex, representing 46.84%, 7.35%, and 45.81% of the study area, respectively. The concave class represents areas where the ground surface curves inward, while the flat class represents areas where the ground surface is relatively flat, and the convex class represents areas where the ground surface curves outward. These classes can be useful in identifying areas where water may accumulate or flow more rapidly, which can have implications for groundwater potential and groundwater detection rates (Fig. 7(h)). The fuzzification of this thematic map involved giving the highest membership values to the concave class and the lowest membership value to the convex class (Fig. 6(g)).

Land Use vs Groundwater Potential

Land use and land cover are important factors in the hydrogeological analysis of an area. This is because groundwater recharge is influenced by land use and land cover (Kaur et al. 2020). Additionally, land use and land cover also affect surface runoff, infiltration, and water percolation. The thematic map generated in Fig. 7(i) is based on a visual interpretation of Sentinel-2A satellite imagery, which has been validated using Google Earth satellite imagery.

In this study, land use and land cover in the study area are divided into seven classes: forest, water bodies, agriculture, shrubs, development, barren land, and cloud cover, each comprising 80.99%, 0.70%, 4.35%, 4.02%, 4.45%, 0.57%, and 4.92% of the study area, respectively. The highest membership value was given to water bodies, followed by agriculture, shrubs, jungle, urban, and barren land, and the lowest membership value was given to cloud cover (Fig. 6(h)).

Porosity vs. Groundwater Potential

Porosity determines a rock's ability to store water (Fajana 2020). In this study, porosity also refers to the volume of open spaces or voids within the rock. Higher porosity allows for more water storage, but not all voids are interconnected, so effective porosity is where voids within the rock are interconnected. Effective rock porosity analysis in the study area is determined using the Skyscan 1275 machine, Bruker Tomography. The porosity values are then incorporated into thematic maps generated using ArcGIS Pro software.

In this study, only rock units with the presence of sandstone are analyzed, considering sandstone's suitability as an efficient aquifer. Three rock samples from the Crocker Formation, Wariu Formation, and Trusmadi Formation were analyzed, each yielding effective porosity percentages of 43.1%, 23.5%, and 21%, respectively. The alluvial unit in the study area is estimated to have a porosity above 46% due to its tendency to store water. The estimated porosity for hard rocks in the study area is below 10%. The porosity in the study area was classified into 5 classes: ≤ 10, $\geq 11 \leq 20$, $\geq 21 \leq 30$, $\geq 31 \leq 45$, and ≥ 46 (Fig. 7(j)). A high membership value was given to the porosity value of the ≥ 46 class, and the lowest membership value was given to the ≤ 10 class (Fig. 6(i)).

Rainfall vs Groundwater Potential

Rainfall distribution in a particular area affects the rate of groundwater recharge. The study area is categorized as a tropical climate area with high annual rainfall, making rainfall distribution a significant factor in groundwater studies. Therefore, rainfall distribution is heavily emphasized in groundwater exploration. Agarwaland & Garg (2016) stated that rainfall distribution affects the amount of water available for infiltration into the groundwater system.

Rainfall distribution data in the study area is based on readings from three weather stations obtained from the Sabah Meteorological Department in the study area. Thematic maps are then generated through interpolation features available in ArcGIS Pro software. Based on the thematic map generated in Fig. 7(k), annual rainfall in the study area is divided into five classes: < 3600mm, 3600mm-3700mm, 3700mm-3800mm, 3800mm-3900mm, and > 3900mm. Areas with the highest rainfall distribution in the study area are concentrated in the western region, while the northeastern region of the study area shows the lowest rainfall distribution. The higher membership value was given to the highest rainfall value, and the lowest membership value was given to the lowest rainfall value (Fig. 6(j)).

TWI vs. Groundwater Potential

The Topographic Wetness Index (TWI) is a humidity index used to assess the topographic control of hydrological processes. It is a function where slope and contributing area per unit orthogonal width to the change in flow direction are involved (Sørensen et al. 2006). The higher the value of the topographic wetness index in an area, the lower the slope. This indicates that the potential for groundwater accumulation in that area is high (Naghibi et al. 2017). The Topographic Wetness Index (TWI) is represented by the following formula;

$$TWI = In\left(\frac{As}{\tan\beta}\right)$$

Where,

As = surface water collection

β = slope of the terrain

The TWI map has been generated using raster DEM data in ArcGIS Pro software through the process of calculating flow direction, flow accumulation, slope, slope to radians conversion, tangent slope calculation, and adjusting flow accumulation. The values of the topographic wetness index in this study have been classified into five classes: <5, 5, 6, 7, and >7 (Fig. 7(i)). For the fuzzification process highest membership value was given to the highest number of twi index values, and the lowest membership value was given to the lowest twi index value (Fig. 6(k)).

Groundwater Potential

The groundwater potential in the study area was divided into five groups of classes: very low, low, moderate, high, and very high. Based on the results, the analysis shows that 32.34% of the study area (274.37 km^2) is categorized as very low groundwater potential, 26.80% of the area (227.37 km^2) as low groundwater potential, 15.55% of the area (131.93 km^2) as moderate groundwater potential, 13.83% of the area(117.33 km^2) as high groundwater potential, and the highest groundwater potential area contributed about 11.48% from the study area (97.40 km^2) (Fig. 8).

The map produced showed that the area with the highest groundwater potential was mostly located at the Crocker

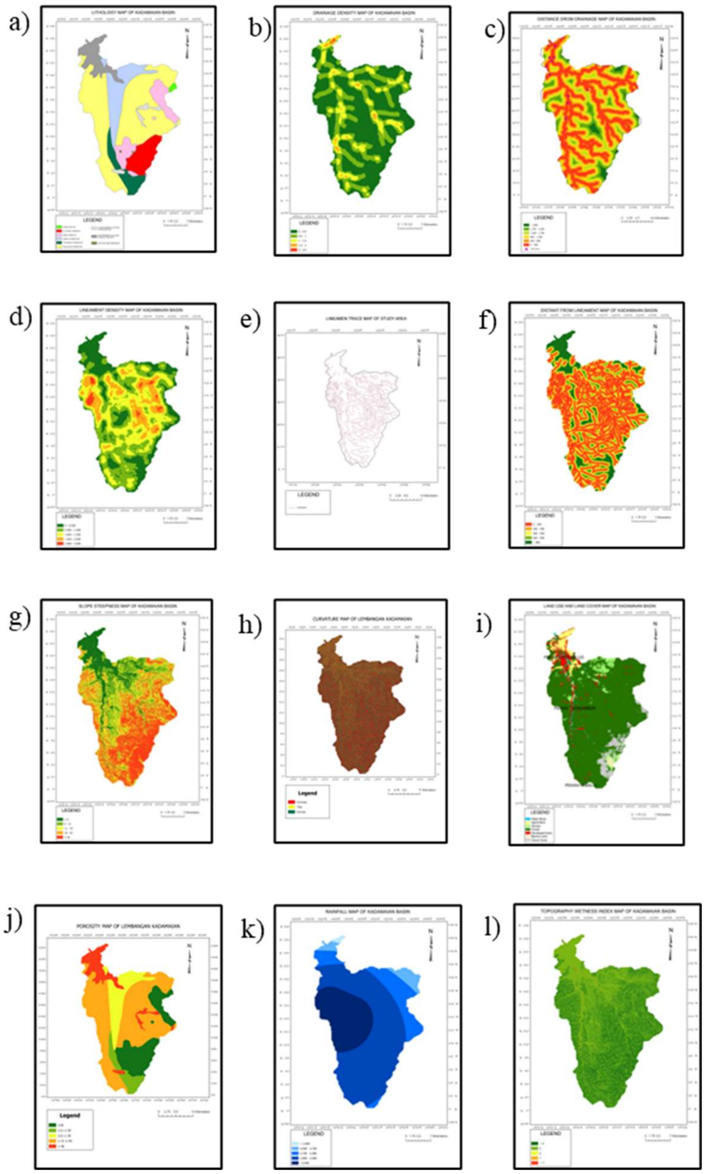

Fig. 7: a) Lithology map b) Drainage Density map c) Distance From Drainage map d) Lineament Density Map e) Lineament Trace map f) Distant From Lineament g) Slope Steepness map h) Curvature map i) Landuse and Land Cover map j) Rock Porosity map k) Rainfall map l) Topography Index map.

formation and Wariu formation, west of the study area and along the Kadamaian River system, which had been estimated to have 11.48% very high and 13.83% high groundwater potential, while alluvium unit, Trusmadi formation, and other hard rock areas such as igneous pluton, basaltic pluton, and basement complex showed a poor groundwater potential. Other than that, based on the groundwater potential map, the very high and high groundwater potential areas were also concentrated in low slope angle areas. Meanwhile, The remaining moderate, low, and very low potential of groundwater, where most of the area can be found at the higher topography area or high slope angle area southeast of the study area. Very high and high potential of groundwater could also be traced near lineaments and drainages. This is because both of the parameters affected the recharge rate of groundwater. Drainage density, however, gave opposite effects from lineament density. High drainage density indicates low permeability in an area that could affect groundwater recharge rate and vice versa for areas with low drainage density, whereas an area with high lineament

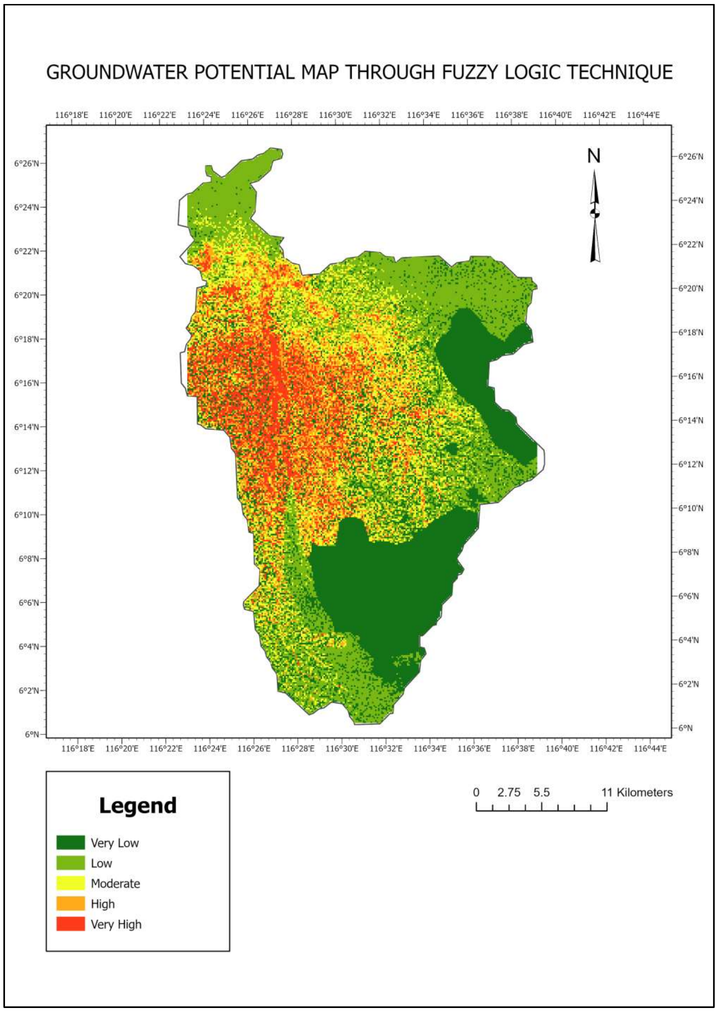

Fig. 8: Groundwater Potential Map in the Lembangan Kadamaian through FLT ROC and AUC Validation of the Groundwater Potential Map.

density indicates a higher recharge rate and low lineament density indicates a lower recharge rate. The very high and high classes also correlate with the rainfall in the study area, where most of the very high and high-value groundwater potential zones can be traced in the high rainfall area west of the study area. Other than that, most of the very high and high potential zones in the study area concentrate in Crocker Formation and Wariu Formation and not in the alluvium unit of the study area, despite having higher estimated porosity than both of the previously mentioned rock units. This was mainly affected by the land use and land cover parameter, where most of the developed areas can be found situated in alluvium units of the study area. Due to high development, developed areas were considered highly polluted and thus were given low membership value. This, however, leads to the outcome of low-potential areas in most of the alluvium units in the study area. The observation on TWI and curvature map, however, doesn't give any visible or directly observable correlation between both its thematic map and groundwater potential zones of the study area. Thus, its effects on groundwater potential can only be explained theoretically.

Both the alluvium and Crocker Formation act as a good aquifer. However, based on the well site datum, most of the high-yield well that exceeds more than 4 m^3/h that were excavated by the Department of Minerals and Geosciences (JMG) was found in the Crocker Formation. Thus it can be concluded that the Crocker Formation is more productive than the alluvium unit of the study area.

However, in this study, the water quality factor of the underground water must be considered to ensure that the water source can be used by the surrounding population. The accuracy of this groundwater potential map was determined by the total well site datum which are the dependent variables of this study.

Table 2: Classification of AUC value ranges.

AUC Value Ranges	Class
0.9 - 1.0	Excellent
0.8 - 0.9	Very Good
0.7 - 0.8	Good
0.6 - 0.7	Fair
0.5 - 0.6	Poor

The method of ROC curve and AUC validation was conducted to assess the effectiveness of the models used in this study. This validation process involves the use of independent data to evaluate how well these models can distinguish between positive and negative classes.

The AUC value ranges between 0.5 and 1.0; the closer the value to 1.0, the higher the accuracy, while the closer the value to 0.5, the lower the accuracy (Fawcett 2006). The relationship between the AUC value and the expected accuracy can be represented by class values in Table 2 (Naghibi et al. 2017).

In this study, a total of 36 existing tube wells within the study area were used in calculating the AUC value to obtain the success rate curve. The AUC value obtained for the logistic regression model is AUC = 0.745 or 74.5% model accuracy (Fig. 9). Based on the AUC value obtained, the Fuzzy Logic Technique can be classified as a good model.

CONCLUSIONS

The research successfully mapped groundwater potential zones in the Lembangan Kadamaian area, Sabah, by employing the Fuzzy Logic Technique as the primary analytical tool, utilizing ArcGIS Pro software for spatial analysis and modeling. The research area, covering approximately 848.4 km², is characterized by geological formations such as Crocker Formation, Wariu Formation, and Pleistocene alluvium deposits, along with other rock units like Trusmadi Formation, basic igneous rocks, crystalline basement, plutonic igneous rocks, and chert-spilite formation. The analysis revealed significant correlations between various parameters and groundwater potential. A total of eleven thematic maps were produced, and each was assigned fuzzy logic membership values and overlaid using a fuzzy toolset in ArcGIS Pro. Lithology, LULC, lineament density, distance from lineaments, drainage density, distance from drainage, and rainfall distribution emerged as crucial factors influencing groundwater occurrence. Areas with sandstone-rich formations, high lineament density, moderate to low drainage density, high to moderate rainfall, less developed, and proximity to drainage and lineament features showed higher groundwater potential. The Fuzzy Logic Technique demonstrated good accuracy (75.2%) in predicting groundwater potential, validated through ROC analysis. The generated groundwater potential map classified the study area into five categories: very high, high, moderate, low, and very low potential zones. The results indicated that around 32.34% of the area had very low potential, while 26.80% had low potential, and 15.55% had moderate potential. Areas with high 13.83% and very high groundwater potential covered approximately 11.48% of the study area, mainly concentrated in the Crocker Formation and Wariu Formation, where each of the classes covered an area of 274.37 km^2, 227.37 km^2, 131.93 km^2, 117.33 km^2, and 97.40 km^2. In addition, the data on the yield rate of tube wells in the study area also, to some extent, help in making comparisons for the existence of groundwater. In addition,

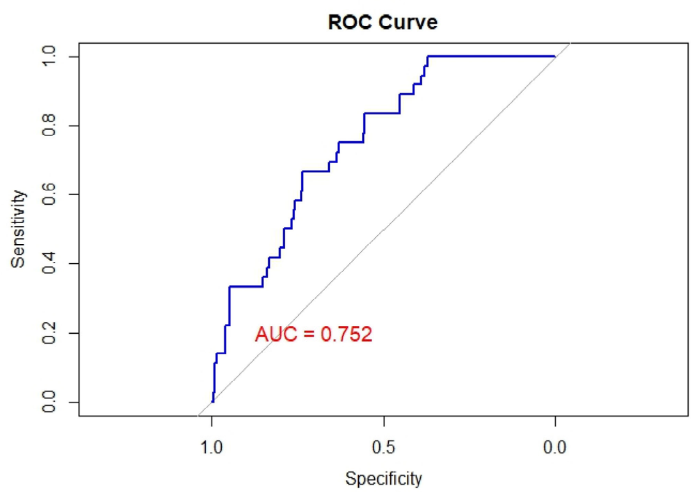

Fig. 9: ROC curve and AUC validation for fuzzy logic technique.

the downside of this model is that it completely abandoned the possibility of groundwater potential in developed areas and doesn't involve the use of field data such as tube well data in its equation of generating groundwater potential zones. However, the findings still contributed valuable observations for sustainable water resource management and land use planning in the region.

ACKNOWLEDGMENT

The authors express appreciation and thank you to Universiti Malaysia Sabah for providing Grant GUG0600-1/2023 and all the support for this study.

REFERENCES

Adeyeye, O.A., Ikpokonte, E.A. and Arabi, S.A., 2019. GIS-based groundwater potential mapping within Dengi area, North Central Nigeria. *The Egyptian Journal of Remote Sensing and Space Science*, 22(2), pp.175-181. DOI.

Agarwal, R. and Garg, P.K., 2016. Remote sensing and GIS-based groundwater potential & recharge zones mapping using multi-criteria decision-making technique. *Water Resources Management*, 30, pp.243–260. DOI.

Al-Ruzouq, R., Shanableh, A., Merabtene, T., Siddique, M., Ali, M., Khalil, M., Idris, A. and Almulla, E., 2019. Potential groundwater zone mapping based on geo-hydrological considerations and multi-criteria spatial analysis: North UAE. *CATENA*, 173, pp.511-524. DOI.

Anteneh, Z.L., Alemu, M.M., Bawoke, G.T., Kehali, A.T., Fenta, M.C. and Desta, M.T., 2022. Appraising groundwater potential zones using geospatial and multi-criteria decision analysis (MCDA) techniques in Andasa-Tul watershed, Upper Blue Nile basin, Ethiopia. *Environmental Earth Sciences*, 81, pp.1-20.

Arulbalaji, P., Padmalal, D. and Sreelash, K., 2019. GIS and AHP techniques based delineation of groundwater potential zones: A case study from Southern Western Ghats, India. *Scientific Reports*, 9, p.2082. DOI.

Assimakopoulos, J.H., Kalivas, D.P. and Kollias, V.J., 2003. A GIS-based fuzzy classification for mapping the agricultural soils for N-fertilizers use. *Science of The Total Environment*, 309(1-3), pp.19-33. DOI.

Balaguru, A., Nichols, G. and Hall, R., 2003. The origin of the circular basins of Sabah, Malaysia. *Geological Society of Malaysia Bulletin*, 46, pp.335-351. DOI.

Basir, D.S., 1988. Barremian radiolaria from Chert-Spilite Formation, Kudat, Sabah. *Sains Malaysiana*, 17(1), pp.67-79.

Benjmel, K., Amraoui, F., Aydda, A., Tahiri, A., Yousif, M., Pradhan, B., Abdelrahman, K., Fnais, M.S. and Abioui, M., 2022. A multidisciplinary approach for groundwater potential mapping in a fractured semi-arid terrain (Kerdous Inlier, Western Anti-Atlas, Morocco). *Water*, 14(10), p.1553. DOI.

Doke, A.B., Zolekar, R.B., Patel, H. and Das, S., 2021. Geospatial mapping of groundwater potential zones using multi-criteria decision-making AHP approach in a hard rock basaltic terrain in India. *Ecological Indicators*, 127, p.107685. DOI.

Fajana, A.O., 2020. Groundwater aquifer potential using electrical resistivity method and porosity calculation: A case study. *NRIAG Journal of Astronomy and Geophysics*, 9(1), pp.168–175. DOI.

Fatin, N.I., Norsyafina, R., Jaineh, L., Umar, H. and Norasiah, S., 2022. Penentuan jenis akuifer di Kota Belud, Sabah menggunakan kaedah seismik pantulan. *Sains Malaysiana*, 51(8), pp.2735-2743. DOI.

Fawcett, T., 2006. An introduction to ROC analysis. *Pattern Recognition Letters*, 27(8), pp.861-874.

Ganapuram, S., Vijaya Kumar, G.T., Murali Krishna, I.V., Kahya, E. and Demirel, M.C., 2009. Mapping of groundwater potential zones in the Musi basin using remote sensing data and GIS. *Advances in Engineering Software*, 40(7), pp.506-518. DOI.

Ghaheri, S., Ismail, M.S., Nasiman, S. and Momeni, M., 2017. Sedimentary architecture and depositional environment of Kudat Formation, Sabah, Malaysia. *IOP Conference Series: Materials Science and Engineering*, 291, p.012025. DOI.

Hung, L.Q., Batelaan, O. and De Smedt, F., 2005. Lineament extraction and analysis, comparison of LANDSAT ETM and ASTER imagery: Case study—Suoimuoi tropical karst catchment, Vietnam. *Proceedings of SPIE*, 5983, p.59830T. DOI.

JMG, 2010. *Garis Panduan Pemetaan Geologi Terain, JMG.GP.06, Kementerian Sumber Asli dan Alam Sekitar*.

Juvanhol, R.S., 2021. GIS and fuzzy logic applied to modeling forest fire risk. *Anais da Academia Brasileira de Ciências*, 93(3), p.e20190726. DOI.

Kaur, L., Rishi, M.S., Singh, G. and Thakur, S.N., 2019. Groundwater potential assessment of an alluvial aquifer in the Yamuna sub-basin (Panipat region) using remote sensing and GIS techniques in conjunction with analytical hierarchy process (AHP) and catastrophe theory (CT). *Ecological Indicators*, 110, p.105850. DOI.

Kollias, V.J. and Kalivas, D.P., 1998. The enhancement of a commercial geographical information system (ARC/INFO) with fuzzy processing capabilities for the evaluation of land resources. *Computers and Electronics in Agriculture*, 20(1), pp.79-95. DOI.

Machiwal, D., Jha, M.K. and Mal, B.C., 2011. Assessment of groundwater potential in a semi-arid region of India using remote sensing, GIS, and MCDM techniques. *Water Resource Management*, 25, pp.1359–1386. DOI.

Magowe, M. and Carr, J.R., 1999. Relationship between lineaments and groundwater occurrence in Western Botswana. *Groundwater*, 37, pp.282-286. DOI.

Mallick, J., Khan, R.A., Ahmed, M., Alqadhi, S.D., Alsubih, M., Falqi, I. and Hasan, M.A., 2019. Modeling groundwater potential zone in a semi-arid region of Aseer using Fuzzy-AHP and geoinformation techniques. *Water*, 11, p.2656. DOI.

Melese, T. and Belay, T., 2022. Groundwater potential zone mapping using analytical hierarchy process and GIS in Muga Watershed, Abay Basin, Ethiopia. *Global Challenges*, 6(1), p.2100068.

Mitra, B., Scott, H.D., Dixon, J.C. and McKimmey, J.M., 1998. Applications of fuzzy logic to the prediction of soil erosion in a large watershed. *Geoderma*, 86(3-4), pp.183-209. DOI.

Naghibi, S.A., Moghaddam, D.D., Kalantar, B., Pradhan, B. and Kisi, O., 2017. A comparative assessment of GIS-based data mining models and a novel ensemble model in groundwater well potential mapping. *Journal of Hydrology*, 548, pp.471-483. DOI.

Ozdemir, A., 2011. GIS-based groundwater spring potential mapping in the Sultan Mountains (Konya, Turkey) using frequency ratio, weights of evidence, and logistic regression methods and their comparison. *Journal of Hydrology*, 411(3-4), pp.290–308.

Poberezhna, L., Shkitsa, L., Poberezhnyi, L., Popovych, P., Brych, V. and Shevchuk, O., 2022. Assessment of environmental risks using elements of fuzzy logic. *2022 12th International Conference on Advanced Computer Information Technologies (ACIT)*, Ruzomberok, Slovakia, pp.219-222. DOI.

Pourghasemi, H., Pradhan, B. and Gokceoglu, C., 2012. Application of fuzzy logic and analytical hierarchy process (AHP) to landslide susceptibility mapping at Haraz watershed, Iran. *Natural Hazards*, 63(2), pp.965–996. DOI.

Pourtaghi, Z.S. and Pourghasemi, H.R., 2014. GIS-based groundwater spring potential assessment and mapping in the Birjand Township, Southern Khorasan Province, Iran. *Hydrogeology Journal*, 22, pp.643–662. DOI.

Razandi, Y., Pourghasemi, H., Neisani, N. and Rahmati, O., 2015. Application of analytical hierarchy process, frequency ratio, and certainty factor models for groundwater potential mapping using GIS. *Earth Science Informatics*, 8, pp.867–883.

Sørensen, R., Zinko, U. and Seibert, J., 2006. On the calculation of the topographic wetness index: evaluation of different methods based on field observations. *Hydrology and Earth System Sciences*, 10(1), pp.101–112. DOI.

Tan, D.N. and Lamy, J.M., 1990. Tectonic evolution of the NW Sabah continental margin since the Late Eocene.

Tesoriero, A.J., Inkpen, E.L. and Voss, F.D., 1998. Assessing groundwater vulnerability using logistic regression. *Proceedings for the Source Water Assessment and Protection 98 Conference*, Dallas, TX, pp.157-165.

Tijia, H.D., 1988. Accretion tectonics in Sabah: Kinabalu suture and East Sabah accreted terrane. *Geological Society of Malaysia Bulletin*, 22, pp.237-251.

Tongkul, F., 1991. Tectonic evolution of Sabah, Malaysia. *Journal of Southeast Asian Earth Sciences*, 6(3-4), pp.395–405. DOI.

Zadeh, L.A., 1996. Fuzzy logic = computing with words. *IEEE Transactions on Fuzzy Systems*, 4(2), pp.103-111.

Zhang, N., Zhou, K. and Du, X., 2017. Application of fuzzy logic and fuzzy AHP to mineral prospectivity mapping of porphyry and hydrothermal vein copper deposits in the Dananhu-Tousuquan island arc, Xinjiang, NW China. *Journal of African Earth Sciences*, 128, pp.84-96. DOI.